Contents lists available at ScienceDirect

Heliyon

journal homepage: www.cell.com/heliyon

Research article

Preparation, characterization, and evaluation of compressive strength of polypropylene fiber reinforced geopolymer mortars

Haci Baykara [a,b,*], Mauricio H. Cornejo [a,b], Andrés Espinoza [b], Enriqueta García [b], Nestor Ulloa [c]

[a] Facultad de Ingeniería Mecánica y Ciencias de la Producción, Escuela Superior Politécnica del Litoral, ESPOL, Campus Gustavo Galindo Km 30.5 Vía Perimetral, Guayaquil, Ecuador
[b] Center of Nanotechnology Research and Development (CIDNA), Escuela Superior Politécnica del Litoral, ESPOL, Campus Gustavo Galindo Km 30.5 Vía Perimetral, Guayaquil, Ecuador
[c] Facultad de Ingeniería, Universidad Nacional de Chimborazo, UNACH, Riobamba, 060102, Ecuador

A B S T R A C T

The study of the fiber-matrix interface represents a crucial topic to determine the mechanical performance of geopolymer-based materials reinforced with polypropylene fibers (PPF). This research proposes the use of natural zeolite in the preparation geopolymers mortars through alkaline activation with NaOH, $Ca(OH)_2$ and Na_2SiO_3, and with river sand as a fine aggregate. PPF were incorporated into the geopolymer-based mortar matrix in different proportions like 0, 0.5, and 1 wt.%. The mortars were cured for 24 h at 60 °C and then aged for six days more at room temperature. All samples analyzed through compressive strength were also characterized by X-ray diffraction, thermal analysis, Infrared Spectroscopy, and scanning electron microscopy techniques. The results indicated that the best mix design among the ones used: NaOH (10 M), $Na_2SiO_3/NaOH = 3$, $Ca(OH)_2 = 1.5$ wt.% and PPF = 0.5 wt.%. The optimum mix design showed a compressive strength of 4.63 MPa on average. Besides, the fibers enhanced the compressive strength of those samples which the PP fibers probably have better dispersion inside the matrix of the geopolymer mortar.

1. Introduction

Traditional Portland cement-based mortars (OPC) are the most widely used materials in the world of construction. This industry is continually facing problems of significant social transcendence in the economic, energetic, and ecological fields due to the high level of production. The most direct damage of OPC production could be related to the amount of the CO_2 emitted. CO_2 is one of the greenhouses gas effects, causing gases. This industry uses large amounts of energy during the processes, which are supplied by burning fossil fuels. It is estimated that for each metric ton of cement, 1.5 MT of raw material is consumed and emitted to the atmosphere 0.8 MT of CO_2 [1].

About 5–7% of total CO_2 emissions in the world are the product of the cement [2, 3]. After all carbon dioxide is one of the main compounds that cause the greenhouse effect [4, 5] which is released to the environment while the limestone reaction ($CaCO_3$) reaches temperatures around 900

°C, being subjected to calcination and causing the formation of calcium oxide and carbon dioxide [6].

OPC-based concrete has many negative impacts that affect its characteristics and properties such as chemical attacks, corrosion, low resistance to high temperatures, cracking, *etc*. [7]. In spite of this, geopolymers and geopolymer based mortars or concretes have advantages for the disadvantages mentioned for OPC and its derivatives [8].

Bhutta et al. [9] used different fibers to reinforce fly ash-based geopolymer mortars. They reported that steel and polyvinyl alcohol fibers could improve both compressive strength and flexural behavior of the geopolymer mortar.

Recently, the life cycle analysis of geopolymers and their derivatives has been reported by various researchers [10, 11]. Passuello et al. [11] studied the life cycle analysis of geopolymer, which are based on kaolin residues from Brazilian mines, indicating that NaOH and sodium silicate productions and thermal curing are the most impacting processes in geopolymer synthesis. Besides, the authors have used a modified rice

husk, which was locally available for the production of sodium silicate and reported that this sodium silicate could reduce the adverse environmental effects at least 60 %.

Punurai et al. [12] replaced the fly ash content with basalt fibers to synthesize hybrid geopolymer paste and evaluate the mechanical properties, microstructure, and drying shrinkage of the paste, resulting in high mechanical strength and decreased drying shrinkage reducing the total porosity and critical pore size of the paste. Likewise, Kheradmand et al. [13] used hybrid polymer fibers to decrease shrinkage in the fly ash-based mortar matrix, obtaining results in reducing shrinkage cracking with only a minimum fiber content of 0.08%, reducing the width of typical crack four times, compared to unreinforced mortars. While Noushini [14] used polypropylene and polyolefin fibers to improve deformation and contraction performance in fly ash-based geopolymer concretes with low calcium contents, obtaining results in the decrease of drying contraction and an increase in the compression creep in the Geopolymer concrete, at both early ages and in the long term, through adding a volume fraction of 0.5% fiber.

On the other hand, the more the plastic industry grows, the more the environmental problems and pollution increases. Especially nondegradable plastics and their macro-, micro or nanoforms jeopardize the life of living organisms. Producers sometimes use fillers for different purposes like to protect the plastic against the UV light, antioxidants, hardeners, plasticizers, etc. One of those fillers is bisphenol A (BPA). According to scientific studies, the BPA affects the reproductive system of the marine creatures, and that is why some fish type may disappear in the future if appropriate actions are not taken [15].

An alternative way to protect the environment, land animals, marine species, and decrease the use of plastics is recycling and use the recycled plastics as reinforcement fibers in the matrix of construction and building materials. There are various studies in the literature using both natural and synthetic nondegradable polymers as reinforcement materials in concrete and geopolymeric structures [16, 17].

Geopolymer cement prepared based on different raw materials have shown promising and similar properties comparing to OPC that is they are considered as an environmentally friendly alternative to OPC [18]. As well-known in the literature, the geopolymers are the products of geopolymerization reaction which the reaction among a raw material rich in silica and alumina such as fly ash [19, 20, 21], blast furnace slags [22, 23, 24] and natural zeolite [25, 26, 27], and an alkaline solution to form a paste that presents characteristics of a binder [28].

Alcantara-Ortega *et al.* [29] used calcium hydroxide to activate natural zeolite (Clinoptilolite) and resulted in a geopolymer mortar with about 38,7 MPa of compressive strength after curing it for 28 days at 50 °C. Villa *et al.* [30] used a mixture of sodium silicate and sodium hydroxide (7 M) solutions to activate a clinoptilolite and heulandite-rich natural zeolite. They have reported that a maximum compressive strength of 33 MPa after curing for 28 days at 40 °C. Nikolov *et al.* [26] prepared clinoptilolite based geopolymers using three different alkaline activators like sodium carbonate, sodium hydroxide, and sodium silicate. The study showed that the best alkaline activator by means of the compressive strength for a curing time of 28 days was sodium silicate (water glass).

There has been a development in construction materials which can provide reinforcement specifically for seismic zones [31] and reduce the formation of internal cracks by plastic retraction due to the drying [18]. For this other kind of fibers like steel [32, 33], polypropylene [18, 34, 35, 36], and natural fiber [37, 38] have been used. In previous studies, the effect that caused fibers of different nature (acrylic and polypropylene) in the tenacity and resistance to the impact of alkaline mortars were analyzed. It was shown that with low fiber content (0.2% v/v), the measured properties are not affected. While with higher fiber content (1% v/v), these values increase. It was also verified that polypropylene fibers improve the impact resistance than acrylic fibers does [18, 33]. Banthia and Gupta [35] reported that reinforcement with PPF up to 0.3%

can improve the mechanical properties of the concrete against the plastic shrinkage and cracks.

Some studies demonstrated that adding a quantity of calcium hydroxide as an extra alkaline activator for the aluminosilicate mass improves the mechanical properties of the yielded geopolymers [39, 40, 41].

In this study, the results of polypropylene fibers-reinforced Ecuadorian natural zeolite based-geopolymer mortars have been presented for the first time. The aim of the PP fiber used as reinforcement materials is to analyze the possibility of the use of recycled plastics in potential reinforcement of geopolymer based mortars. Different quantities of polypropylene fiber have filled the geopolymer mortars (by wt.% of 0, 0.5 and 1) and varying amounts of calcium hydroxide (by wt.% 0.5, 1.0 and 1.5) with respect to the mass of zeolite rich tuff used.

2. Materials and methods

2.1. Raw materials

The Ecuadorian zeolite-rich tuff was supplied by INDAMI SA, whose particle size was mainly ~200 μm. The tuff was dried at 80 °C for 24h in a laboratory oven, then its particle size reduced to less than 45 μm by a ball miller. Samples of the tuff were analyzed by quantitative X-ray diffraction (XRD) showing its mineralogical composition as can be seen in Figure 1. The XRD results of the sample analyzed after a milling process showed that the zeolite-rich tuff is mainly composed of the minerals like mordenite (~9%), calcite (~23 %), quartz (~20%) and amorphous content (~48%).

The geopolymer mortars were prepared using natural zeolite rich-tuffs and river sand collected from the banks of the Pastaza River. This sand was carefully obtained to avoid impurities and washed its use in geopolymer mortar preparation. Besides, the sand was dried at 80 °C for 24h, then sieved by ASTM mesh between No. 30 and 40. XRD was used to elaborate the mineralogical composition of the sand, and the results are as follows (see Figure 1): anorthite (~0.2%), albite (~74 %), quartz (~11%), amorphous content (~4%).

Alkaline activators were selected based on previous articles that showed good values of compressive strength [42, 43, 44]. NaOH (Merck) with a purity of 99%, Na_2SiO_3 (Merck) with specifications: Na_2O between 7.5 and 8.5%, and SiO_2 between 25.5 and 28.5. $Ca(OH)_2$ with a purity of 96%. Since the solubility of $Ca(OH)_2$ is very low, it was used as the solid additive with varying amounts 0.5–1.5 wt.% with respect the mass of the raw material used (see Table 1).

Commercially available polypropylene fibers (PPF), 150-e3 (provenance with a length of ~12–19 mm) have been used to be evaluated whether it affects the mechanical properties mainly compressive strength of geopolymer mortars or not.

2.2. Synthesis, testing, and characterization

The zeolitic tuff and fine aggregates were mixed manually for 5 min then activated by using different alkaline solutions of NaOH (10 M) and Na_2SiO_3 to synthesize geopolymer mortar. These solutions were prepared in proportions of $Na_2SiO_3/NaOH = 3$. Also, they were mixed with varying percentages of $Ca(OH)_2$ such as 0.5, 1.0, and 1.5 wt.% zeolitic tuff, and PPF, 0, 0.5 and 1.0 wt.%. All specimens were prepared with a constant ratio of liquid to solid (activator/zeolite = 0.5) and a constant rate of sand/zeolite = 1.5. For all samples, an extra amount of water of 26 mL was added to keep workability steady. The raw materials were mixed for 3 min up to get a homogeneous mixture. Then the mixture was cast in cubic molds of 5 cm^3 following the standard ASTM C109/C109 M-16a [45], for the compressive strength test (see Figure 2). Samples were cured in the molds for 24 h at 60 °C, covered with a plastic bag to prevent rapid dehydration and possible drying-shrinkage of the mortars [46]. Afterward, these samples were demolded and kept at room temperature and conditions (on average 25.4 °C and 50.1% relative humidity) for six days
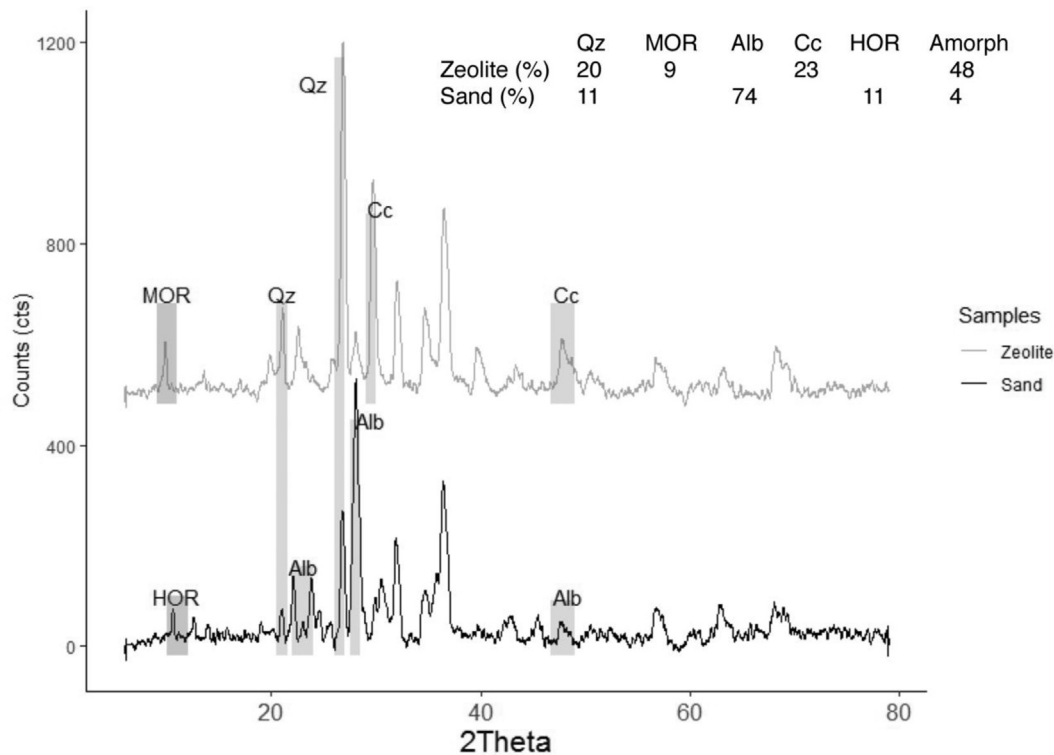
Figure 1. Quantitative XRD analysis of raw materials, natural zeolite rich tuff, and river sand.

Table 1. Mixing design for geopolymer mortar synthesis.

Mix ID	Activator/zeolite ratio	Na$_2$SiO$_3$/NaOH ratio	River Sand (g)	Zeolite (g)	Ca(OH)$_2$ (wt.%)	PP fiber (wt.%)
GM-05-0	0.5	3	135	90	0.5	0
GM-1-0	0.5	3	135	90	1	0
GM-1.5-0	0.5	3	135	90	1.5	0
GM-05-05	0.5	3	135	90	0.5	0.5
GM-1-05	0.5	3	135	90	1	0.5
GM-1.5-05	0.5	3	135	90	1.5	0.5
GM-05-1	0.5	3	135	90	0.5	1
GM-1-1	0.5	3	135	90	1	1
GM-1.5-1	0.5	3	135	90	1.5	1

GM- Geopolymer Mortar; 0.5–1.5: Ca(OH)$_2$ content, 0–1: PPF content.

more before the compressive strength tests. Three samples of each composition were prepared (See Table 1 for the details of each mix design).

Compressive strength test was performed for three mortar specimens of each composition, these tests were run in the equipment SHIMADZU ® model UTM-600KNI, based upon standard ASTM C109/C109 M-16a [45].

Like for raw materials, geopolymer mortars are characterized by quantitative X-ray diffraction using PANanalytical ® model X'pert. The samples were prepared as follows. First, fractured pieces of geopolymer mortar from compressive strength tests were collected. The collected samples were milled by using pestle and mortar up to an average size of 45 μm. Then an aliquot of 0.6 g was picked up and then mixed with 0.06 g (10% sample wt.%) of ZnO, the internal standard. The operating conditions were: 45 kV; 40 mA and scanning range of 5–80 (°2Theta) with step size 0.02° to 2 s of scan time per step, using a conventional X-ray tube (Cu_Kα radiation) and a multi-channel X'Celerator detector with anti-scatter protection. HighScore Plus ® software was used for the quantification of the mineralogical composition of each sample.

The thermal behavior and the thermal stability analysis of both raw materials and geopolymer mortars were carried out using a TA® Instruments Q-600 equipment, simultaneous thermal analyzer STD. For this analysis, the samples were milled by using pestle and mortar up to an average particle size of 45 μm. Then an aliquot of approximately 10–15 mg was picked up and then poured into alumina crucibles. The operating conditions were nitrogen flow 100 mL/min, the heating ramp of 20 °C/min at a temperature ranged from room temperature to 1000 °C.

A Perkin Elmer Spectrum 100 model spectrophotometer was used to determine the main functional groups in the geopolymer mortars. For this purpose, the KBr pellet method has been used, and the samples were analyzed in the range of 4000–400 cm^{-1} with an average of 10 scans.

Morphology and the degree of geopolymerization (concerning the increase of amorphous content) of the geopolymer mortars specimens were studied using an Inspect S model FEI® scanning electron microscope equipped with an Energy Dispersive Spectrometer (EDS). Operating conditions used were as follows high vacuum, a pressure of 12 Pa, an acceleration voltage of 14 kV and 3 as spot size.
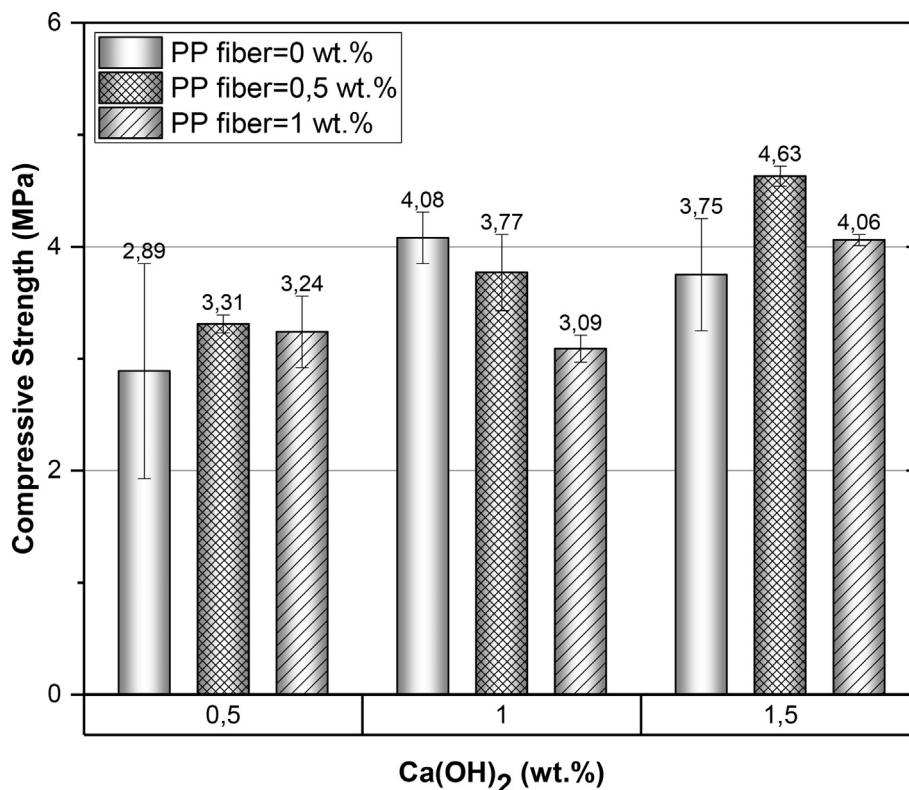
Figure 2. The compressive strength of natural zeolite-based geopolymer mortars.

3. Results and discussion

3.1. Compressive strength

The effect of calcium hydroxide content on the compressive strength of geopolymer mortars at an early age (i.e., seven days) are shown in Figure 2. The mechanical performance of the samples varied according to the percentage of PPF and the amount of $Ca(OH)_2$ were used in the matrix of the geopolymer mortars. As seen in Figure 2, the compressive strength of the composite material reinforced with 0.5 wt.% PPF and 1.5 wt.% $Ca(OH)_2$ presents a considerable increase in the compressive strength compared to the other samples, while there was an adverse effect on the mechanical performance of the compounds with the highest amount of polypropylene fibers (>1 wt.%). Similar results were reported in other investigations related to fly ash-based geopolymer mortars [47, 48]. It was observed that there is an association between the addition of fraction/volume of PPF and the low mechanical performance in the compounds reinforced with PPF. The same adverse effect related to a higher amount of PPF has been observed in our study as well. This adverse effect is probably due to the not homogenous distribution and agglomeration of PP fiber inside the geopolymer mortar matrix. The less workability of geopolymer mortars consequently would lead the decrease in collision of the reactants which cause the formation of geopolymer cement. However, the reduction in workability of the fresh, composite matrix could also be caused by the $Ca(OH)_2$ content that contributes to the adverse effect of workability. It could be one cause for complications at the moment of compaction in the molds, thus forming cracks over the surface of geopolymer samples. As can be seen in Figure 2, as the percentage of PPF increases, the mechanical resistance decreases, and this agrees with the low workability that the mixtures present.

One of the most critical impacts of fiber reinforcement is preventing the significant deformation of the mortars. As clearly seen in Figure 4, the compactness of the mortar samples with and without the reinforcement after the compressive strength tests. So, the fibers give high structural stability to the geopolymer mortars. The samples without the reinforcement are demolished, but the samples with PPF reinforcement are compact without destruction.

In summary, the geopolymer mortar showed the highest compressive strength was that of NaOH (10 M), Na_2SiO_3/NaOH = 3, $Ca(OH)_2$ = 1.5 wt.% and PPF = 0.5 wt.%. These reinforcement mortars did not present cracks on the surface, and after compressive strength tests, these samples with reinforcement did not break completely (see Figure 3).

3.2. X-ray diffraction analysis (XRD)

The quantitative X-ray diffraction using Rietveld refinement method was done to all geopolymer mortars and raw materials. The zeolitic tuff used a solid precursor was composed of mordenite (~9 %), calcite (~23%), quartz (~20%), amorphous content (~48%). In the case of sand, it was mainly composed of albite (~74%), quartz (~11%), amorphous content (~4%), and Hornblende (HOR) (11%) as the secondary phase. The mineralogical composition of geopolymer mortars grouped by PP fiber content is shown in Figures 4, 5, 6, and 7. As a result, calcite, quartz, and albite kept almost constant (see Figure 4.) their original substances after alkaline activation regardless of the amount of PPF. This result suggests that those minerals did not take part in the geopolymerization reaction. It is well known the inert character of quartz and albite [40] as reported in previous studies. The solubility of in the reaction ambient calcite depends on the level alkalinity. Some researchers reported that calcite showed low reactivity in such systems; although its reactivity increases when the alkalinity decreases [49, 50].

The natural zeolites, mordenite, and clinoptilolite, unlike the Albite, quartz, and calcite showed different behavior in the reaction. Their contents decreased after seven days of reaction; in fact, the only mordenite was able to be detected by X-ray diffraction. This result suggests that both mordenite and clinoptilolite took place and consumed as the source of alumina and silica for geopolymerization transforming into amorphous content in the geopolymeric matrix.
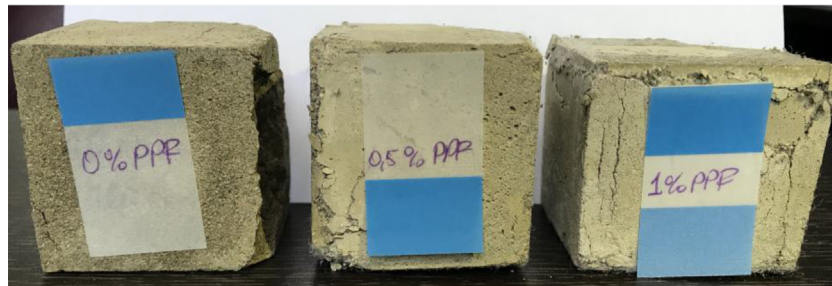
Figure 3. The difference between reinforced and non-reinforced blocks after the compressive strength test.
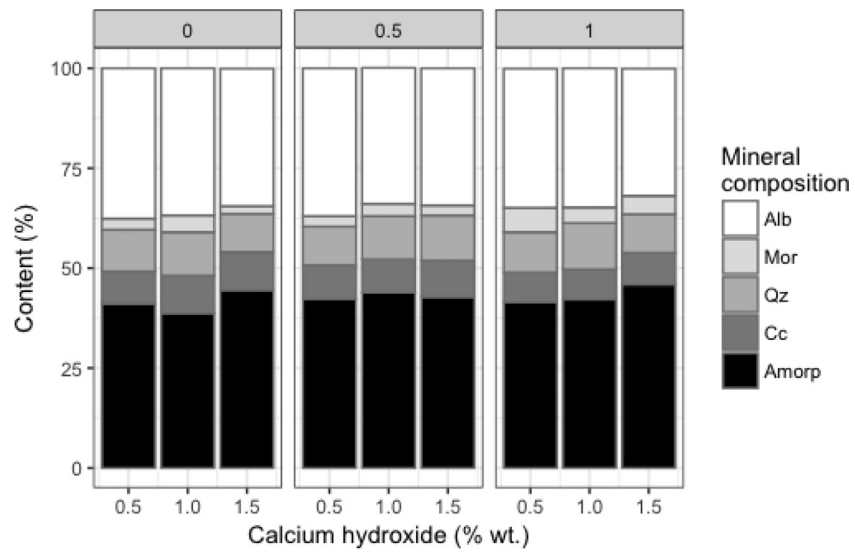

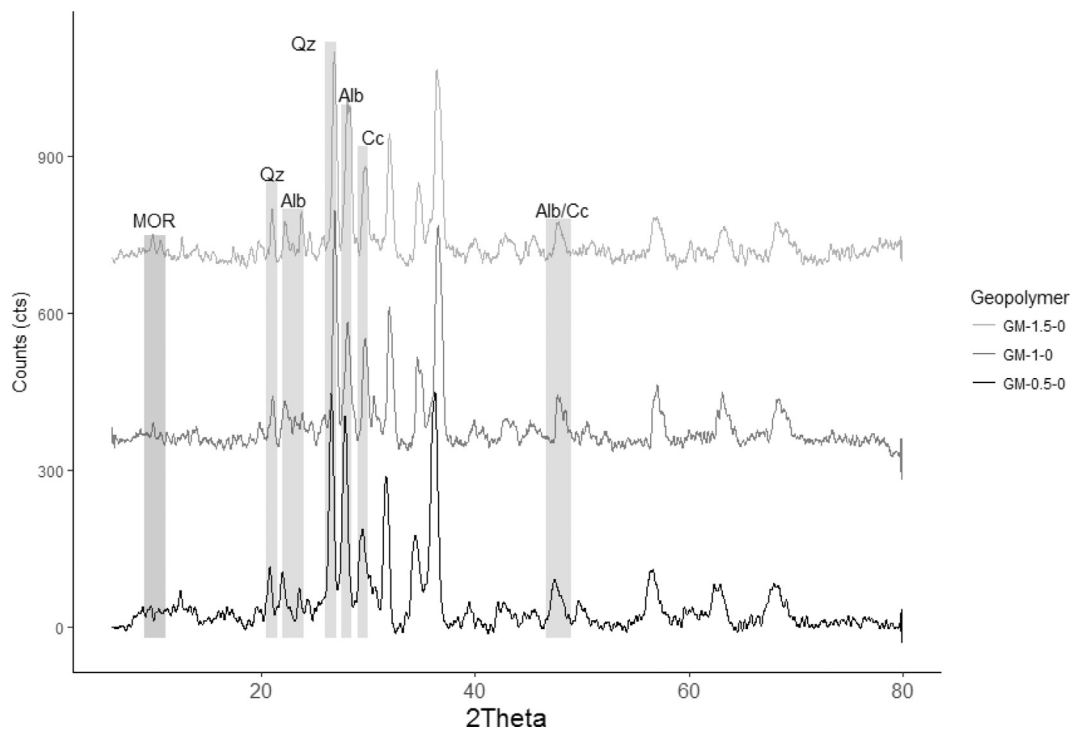**Figure 4.** Mineral composition of the geopolymer mortars elaborated by QXRD.

Figure 5. QXRD analysis of the geopolymer mortars different amounts of $Ca(OH)_2$ and without reinforcement with PPF.
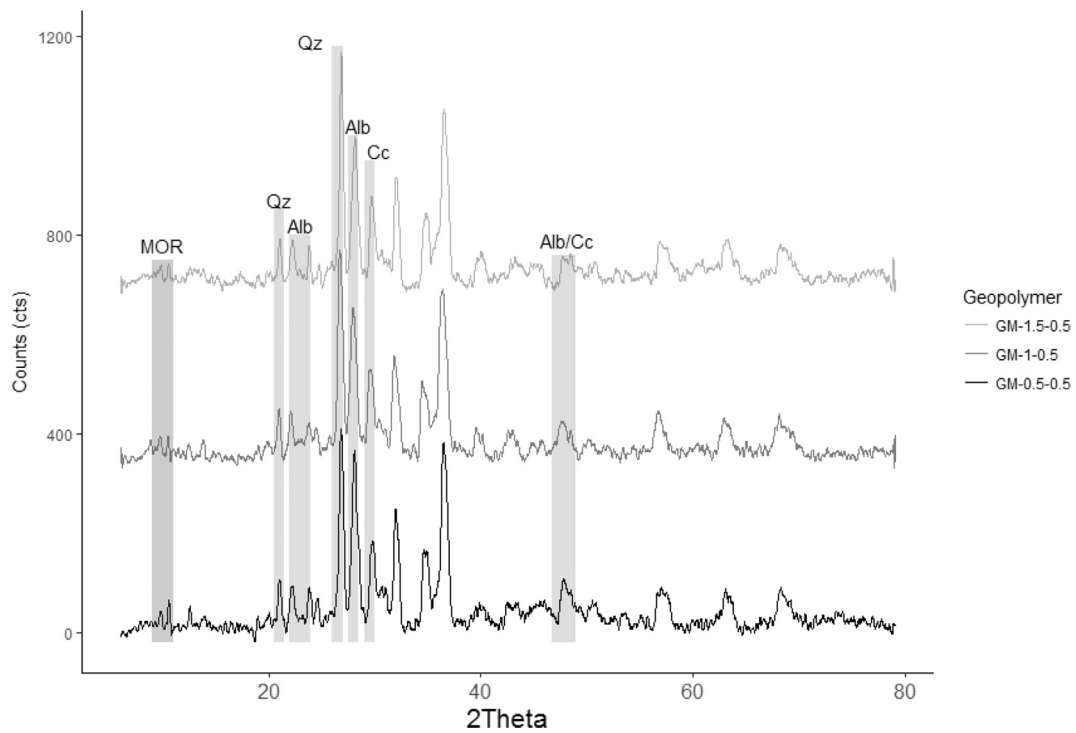
Figure 6. QXRD analysis of the geopolymer mortars with 0.5 wt.% PPF and different amounts of Ca(OH)$_2$.
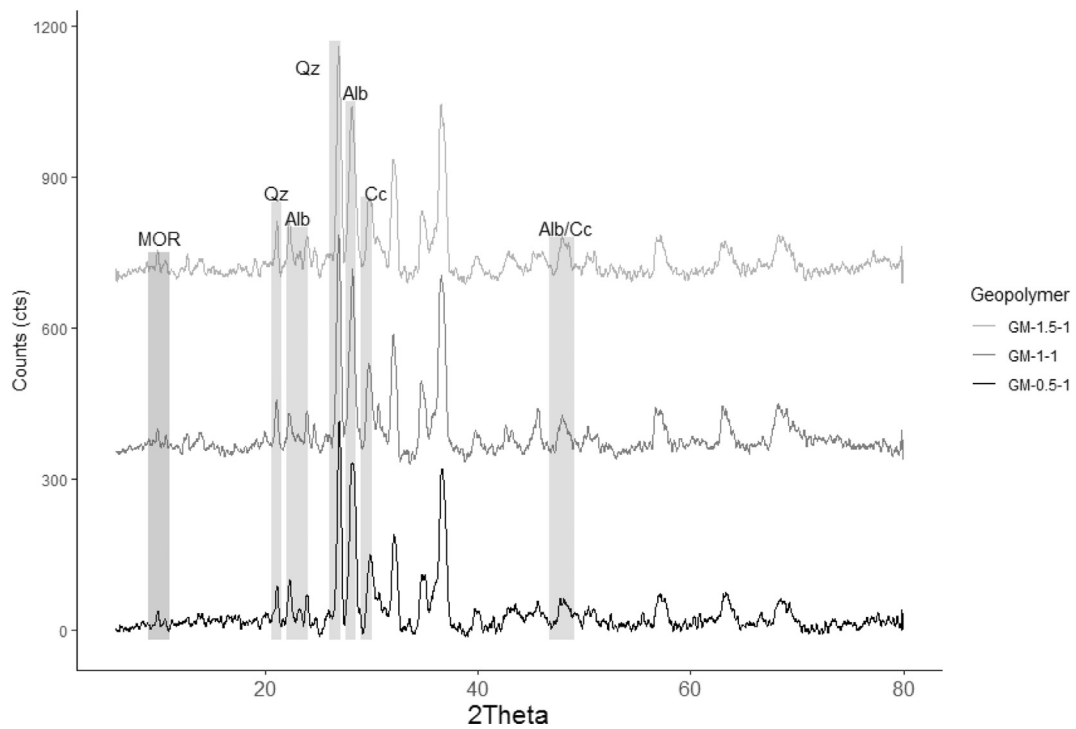

Figure 7. QXRD analysis of the geopolymer mortars with 1 wt.% PPF and different amounts of Ca(OH)$_2$.

Among geopolymer mortars, the contents of amorphous were similar after seven days of reaction. The amorphous content can be considered as one criterion of evaluation of the reaction degree.

3.3. Morphological analysis by SEM-EDS

Figure 8 shows the SEM micrographs of the geopolymer mortars with and without PPF reinforcement in which a significant amount of amorphous content can be observed. All series showed more compact matrix as the content of calcium hydroxide increased regardless of the amount of PP fiber. The compact and amorphous matrix is mostly related to the geopolymeric structure and probably to the calcium silicate, which forms during geopolymer mortar preparation. The reason for the decreasing of workability with the increase of the amount of the Ca(OH)$_2$ is due to the formation of solid CaO.SiO$_2$. The geopolymer gel gets solidified by the addition of Ca(OH)$_2$ to the mixture and the formation of
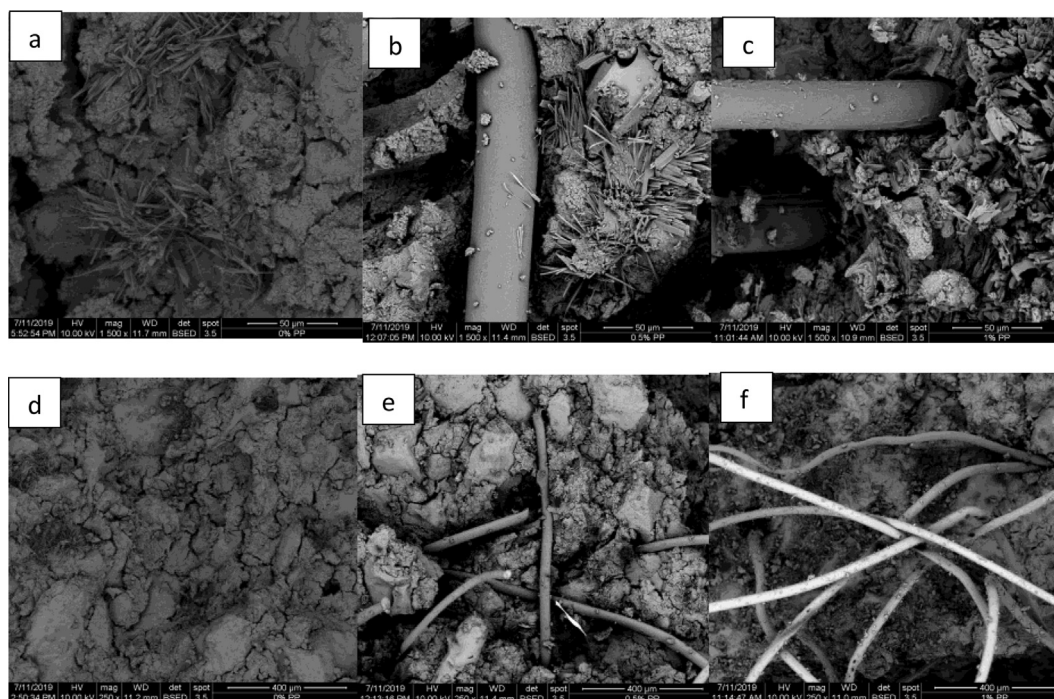
Figure 8. SEM micrographs of the samples of geopolymer mortar samples, a,d) PPF = 0 wt.%. with Ca(OH)$_2$ = 0.5 wt.%, b,e) PPF = 0.5 with Ca(OH)$_2$ = 1 wt.%. and c,f) PPF = 1.5 with Ca(OH)$_2$ = 1,5 wt.% with different magnifications.

CaO.SiO$_2$ give a short term strength and hardness. The reaction is between calcium hydroxide and sodium silicate, forming the salt mentioned above.

As seen in the Figure 8, there are some particles which can be attributed to unreacted zeolite within the geopolymer matrix, albite from sand and possible carbonates like CaCO$_3$ and Na$_2$CO$_3$ possibly formed due to the reaction between alkaline activators and the CO$_2$ during the curing time. Some researchers [33, 47, 48, 51] reported that unreacted particles within the geopolymeric matrix led to low values of compressive strength. Mainly Na$_2$CO$_3$ can be formed in both with and without PPF reinforced geopolymer mortars due to the reaction of NaOH with CO$_2$ (see fiber-like formations in a, b and c images in Figure 8.). Those fiber-like formations are the crystals of Na$_2$CO$_3$, and it is proved by semi-quantitative SEM-EDS as well (see Fig. S5. in Supplementary file). The experimental elemental analysis of those crystalline phases obtained by SEM-EDS is very close to the theoretical elemental analysis of Na$_2$CO$_3$. As seen in Figure 8, reinforced geopolymer mortars have Na$_2$CO$_3$ formed around the fibers. That type of carbonates is probably due to the channels formed, which are due to the least interaction between the nonpolar structure of PPF and polar structure of geopolymeric matrix. So, it can be estimated that CO$_2$ molecules migrated through those channels inside the geopolymer matrix and reacted with alkaline activators forming carbonates. Recent literature shows that carbonation has a positive impact on the durability of natural fiber reinforced cementitious composites, increase the strength, and decrease water absorption by increasing the density [52].

Figure 8 (b,c,e and f images) shows the smooth surface of PP fiber and its original shape remained. It seems that there was not any chemical degradation of PPF and it doesn't have a chemical bonding with the aluminosilicate matrix, thus forming a less resistant geopolymer mortar reinforced with higher PPF content [48]. Similar studies [47, 48] agreed with these results suggesting that the shape and smooth appearance of PPF fibers explained the low mechanical performance of geopolymers reinforced with PPF.

The effect of hydrophobicity and the contraction that occurs in the fiber-matrix interaction of the reinforced composites with PPF can explain the low compressive strength observed in such materials. PP

fibers behave as a hydrophobic material that originates from its nonpolar chemical structure and its nanoscale corrugated roughness. Therefore, the PPF has the effect of repelling water [48, 53] which means that it does not absorb water, and harm the drying of the geopolymer matrix. This effect can produce air bubbles trapped between the grooves of the surface of the fibers and the geopolymer mortar. Also, geopolymer compounds shrunk over time, that implies the formation of internal stress in the specimens, thus resulting in the detachment of the fibers from the geopolymeric matrix [48].

3.3.1. Thermogravimetric analysis and differential scanning calorimetry (TGA/DSC)

Table 2 shows the results of the weight loss as temperature rises for all samples. In summary, the effect of PPF and Ca(OH)$_2$ on the weight loss of geopolymer mortars with and with PPF was meaningless. In this table, there was a significant loss of mass between 25 and 100 °C. That mass loss is attributed to the evaporation of pore water, and it is due to short-term curing conditions (7 days) and can be reduced under long-term curing conditions [54, 55]. The mass loss in the range of 100–300 °C is attributed by the loss of the intermolecular and crystalline water exist in the geopolymer structure. An additional mass loss is observed in the range of 300–500 °C, which is attributed to the dehydroxylation of the Si–OH and Al–OH groups presented in the geopolymer mortars [54, 56]. It is also due to the loss of fiber polypropylene which degrades in the temperature range between 400-500 °C, as seen in Fig. S1 (in Supplementary file).

The highest percentage of mass loss for all samples is in the temperature range of 500–750 °C. This mass loss can be attributed to the decarbonization of carbonates naturally included in the zeolite, and potential byproducts such as CaCO$_3$ and Na$_2$CO$_3$ formed due to the excess of activator used and CO$_2$ [54].

Fig. S3 (in Supplementary file) shows overlaid DSC plots of all samples in which can be seen that all the samples are presenting similar characteristics. Two characteristic peaks are observed in all thermograms; one or two endothermic peaks at low temperatures and one exothermic peak at higher temperatures. Concerning heat flow, water evaporation, dehydroxylation, and carbonation processes are

Table 2. Thermogravimetric analysis of the geopolymer samples and PP fiber.

Mix ID	Temperature range (°C)/Mass loss (%)			
	RT-250	250–500	500–800	RT-1000
GM-0.5-0	5,06	2,13	4,1	11,71
GM-1-0	3,01	1,41	4,26	8,92
GM-1.5-05	3,15	1,63	3,98	9,07
GM-0.5-05	3,52	2,01	3,66	9,32
GM-1-05	3,08	2,98	3,80	10,11
GM-1.5-05	4,93	1,93	3,97	11,16
GM-0.5-1	3,02	2,52	3,83	9,60
GM-1-1	3,14	2,49	3,63	9,52
GM-1.5-1	2,984	2,69	3,58	9,53
PPF	1 (melting 160)			

RT: Room Temperature.

endothermic reactions. The endothermic peak in the DSC thermograms lies in the range between room temperature and 200 °C, and this was attributed to the evaporation of free water in the geopolymer structure, as mentioned before. Starting at 750 °C, DSC plots showed the onset of the exothermic phenomenon. This peak could be caused by the recrystallization or reorganization of phases found in the samples, which can form new phases at such high temperatures [54, 56]. According to Table 2, these geopolymer mortar can be considered as thermostable from approximately 750 °C, where a total average mass loss of 11.61% (see Table 2) was observed.

3.4. Fourier transform infrared spectroscopy FTIR

Table 3 presents the assignments of the FTIR spectra (See Fig. S4. in Supplementary file) of the geopolymer samples that showed the highest compressive strength. One of the most prominent peaks is the one that is at the wavenumber between 3467-3434 cm^{-1}, which corresponds to the stretching vibration O–H (in hydroxyl groups) in water molecules or geopolymer structure. The existence of hygroscopic water is confirmed by peaks observed at 1645-1638 cm^{-1}, which is due to the bending vibration water molecules inside the amorphous structure of the geopolymer mortars [55]. The peaks observed between approximately 3000–2800 cm^{-1} are due to the presence of CH$_2$ groups, mainly due to the presence of polypropylene in the mixture of the matrix of the geopolymer mortar. The peak observed between the wavenumber of 1455 and 1426 cm^{-1} is due to the stretching vibration of O–C–O, which is due

to the formation of calcium carbonate and sodium carbonates [55]. The least significant peaks are found in the wavenumbers between 1041 and 1031cm^{-1}, due to the asymmetric vibration of the Si–O–Si and Al–O–Si groups, and between 799 and 610 cm^{-1} which is due to the symmetric stretching vibration of the Al–O bonds. These peaks are the evidence for the formation of the geopolymer is likely produced due to the dissolution of the silicates and aluminates presented in the zeolite rich tuffs which can be dissolved in the alkaline solution [26].

4. Conclusions

In this research, the polypropylene fiber and zeolite-based geopolymer mortar matrix interaction and the effect of Ca(OH)$_2$ on mechanical performance and thermal stabilities of the mortars have been studied.

The best mix design with respect to the maximum compressive strength obtained was: Na$_2$SiO$_3$/NaOH (10 mol/L)) = 3, Ca(OH)$_2$ = 1.5 wt.% and PPF = 0.5 wt.%.

The PPF can improve the compressive strength of the samples which have been cured for seven days. On the other hand, incorporation of PPF enhances the compactness of geopolymer mortars when the samples are under a force comparing to the samples without the reinforcement.

Since the PPF has advantages as reinforcement material in the matrix of zeolite-based geopolymer mortar matrix, these types of plastics/ polymers could be considered for the recycled and evaluated for potential use in the construction and civil engineering industry.

Table 3. Frequencies of the absorption bands (cm^{-1}) taken from the spectra (Fig. S4. in Supplementary file) of the geopolymer samples.

Mix ID	Wavenumber (cm^{-1})					
	Assignment					
	O–H stretching vibration	H–O–H molecular bending	C–O (sodium, calcium) carbonates stretching mode	Si–O-T (T = Si, Al; where Si and Al are tetrahedral), and asymmetric stretching, O–C–O stretching mode	Si–O–Si bond (presence of quartz), symmetric stretching	Si–O–Si/Al–O–Si, symmetric stretching, or C–O out of plane bending
GM-0.5-0	3467	1642	1432	1031	797	714
GM-1-0	3460	1640	1428	1035	798	713
GM-1.5-05	3437	1641	1428	1035	798	713
GM-0.5-05	3439	1639	1431	1039	798	711
GM-1-05	3438	1638	1437	1035	798	714
GM-1.5-05	3434	1640	1450	1035	798	713
GM-0.5-1	3462	1641	1438	1040	798	714
GM-1-1	3437	1641	1435	1036	798	714
GM-1.5-1	3437	1641	1455	1031	796	713

Declarations

Competing interest statement

The authors declare no conflict of interest.

Additional information

Supplementary content related to this article has been published online at https://doi.org/10.1016/j.heliyon.2020.e03755.

References

[1] A. Fernández-Jiménez, A. Palomo, Propiedades y aplicaciones de los cementos alcalinos, Rev. Ing. Constr. 24 (2009) 213–232.

[2] B.C. McLellan, R.P. Williams, J. Lay, A. Van Riessen, G.D. Corder, Costs and carbon emissions for geopolymer pastes in comparison to ordinary portland cement, J. Clean. Prod. 19 (2011) 1080–1090.

[3] A. Bosoaga, O. Masek, J.E. Oakey, CO2 capture technologies for cement industry, Energy Proc. (2009) 133–140.

[4] A.R. Sakulich, Reinforced geopolymer composites for enhanced material greenness and durability, Sustain. Cities Soc. 1 (2011) 195–210.

[5] M.H. Al-Majidi, A. Lampropoulos, A.B. Cundy, Tensile properties of a novel fibre reinforced geopolymer composite with enhanced strain hardening characteristics, Compos. Struct. 168 (2017) 402–427.

[6] I.E.A. IEA, Tracking Industrial Energy Efficiency and CO2 Emissions, 2007.

[7] M. Eglinton, Resistance of concrete to destructive agencies, Lea's Chem. Cem. Concr. (2003) 299–342.

[8] M. Vafaei, A. Allahverdi, Acid-resistant geopolymer based on fly ash–calcium aluminate cement, J. Mater. Civ. Eng. 30 (2018) 4018143.

[9] A. Bhutta, P.H.R. Borges, C. Zanotti, M. Farooq, N. Banthia, Flexural behavior of geopolymer composites reinforced with steel and polypropylene macro fibers, Cem. Concr. Compos. 80 (2017) 31–40.

[10] D.A. Salas, A.D. Ramirez, N. Ulloa, H. Baykara, A.J. Boero, Life cycle assessment of geopolymer concrete, Constr. Build. Mater. 190 (2018) 170–177.

[11] A. Passuello, E.D. Rodríguez, E. Hirt, M. Longhi, S.A. Bernal, J.L. Provis, A.P. Kirchheim, Evaluation of the potential improvement in the environmental footprint of geopolymers using waste-derived activators, J. Clean. Prod. 166 (2017) 680–689.

[12] W. Punurai, W. Kroehong, A. Saptamongkol, P. Chindaprasirt, Mechanical properties, microstructure and drying shrinkage of hybrid fly ash-basalt fiber geopolymer paste, Constr. Build. Mater. 186 (2018) 62–70.

[13] M. Kheradmand, Z. Abdollahnejad, F. Pacheco-Torgal, Drying shrinkage of fly ash geopolymeric mortars reinforced with polymer hybrid fibres, Proc. Inst. Civ. Eng. Constr. Mater. 173 (2020) 28–40.

[14] A. Noushini, A. Castel, R.I. Gilbert, Creep and shrinkage of synthetic fibre-reinforced geopolymer concrete, Mag. Concr. Res. 71 (2019) 1070–1082.

[15] R. Stafford, P.J.S. Jones, Viewpoint – ocean plastic pollution: a convenient but distracting truth? Mar. Pol. (2019), 0–1.

[16] Y. Wang, H.C. Wu, V.C. Li, Concrete reinforcement with recycled fibers, J. Mater. Civ. Eng. 12 (2000) 314–319 (2000)12:4(314).

[17] Z. Li, R. Chen, L. Zhang, Utilization of chitosan biopolymer to enhance fly ash-based geopolymer, J. Mater. Sci. 48 (2013) 7986–7993.

[18] F. Puertas, T. Amat, A. Fernández-Jiménez, T. Vázquez, Mechanical and durable behaviour of alkaline cement mortars reinforced with polypropylene fibres, Cem. Concr. Res. 33 (2003) 2031–2036.

[19] J. Davidovits, Geopolymer Chemistry and Applications, fourth ed., Institut Géopolymère, 2008.

[20] J.L. Provis, J.S.J. Van Deventer, Geopolymers: Structures, Processing, Properties and Industrial Applications, 2009.

[21] R. Dirgantara, C. Gunasekara, D.W. Law, T.K. Molyneaux, Suitability of Brown coal fly ash for geopolymer production, J. Mater. Civ. Eng. 29 (2017) 4017247.

[22] H. Wan, Z. Shui, Z. Lin, Analysis of geometric characteristics of GGBS particles and their influences on cement properties, Cem. Concr. Res. 34 (2004) 133–137.

[23] P. Duxson, J.L. Provis, Designing precursors for geopolymer cements, J. Am. Ceram. Soc. 91 (2008) 3864–3869.

[24] M.A. El-Wafa, K. Fukuzawa, Early-age strength of alkali-activated municipal slag–fly ash–based geopolymer mortar, J. Mater. Civ. Eng. 30 (2018) 4018040.

[25] J.L. Villalba, J. Macías, H. Baykara, N. Ulloa, G. Soriano, Operational energy comparison of concrete and foamed geopolymer based housing envelopes, ASME Int. Mech. Eng. Congr. Expo. Proc. (2017).

[26] A. Nikolov, I. Rostovsky, H. Nugteren, Geopolymer materials based on natural zeolite, Case Stud. Constr. Mater. 6 (2017) 198–205.

[27] L. Machiels, D. Garcés, R. Snellings, W. Vilema, F. Morante, C. Paredes, J. Elsen, Zeolite occurrence and genesis in the Late-Cretaceous Cayo arc of Coastal Ecuador: evidence for zeolite formation in cooling marine pyroclastic flow deposits, Appl. Clay Sci. 87 (2014) 108–119.

[28] F. Pacheco-Torgal, J.A. Labrincha, C. Leonelli, A. Palomo, P. Chindaprasirt, Handbook of Alkali-Activated Cements, Mortars and Concretes, Woodhead Publishing Limited, 2014.

[29] E.A. Ortega, C. Cheeseman, J. Knight, M. Loizidou, Properties of alkali-activated clinoptilolite, Cem. Concr. Res. 30 (2000) 1641–1646.

[30] C. Villa, E.T. Pecina, R. Torres, L. Gómez, Geopolymer synthesis using alkaline activation of natural zeolite, Constr. Build. Mater. 24 (2010) 2084–2090.

[31] P. Sarker, M. Begum, S. Nasrin, Fiber reinforced polymers for structural retrofitting: a review, J. Civ. Eng. 39 (2011) 49–57.

[32] A. Islam, U.J. Alengaram, M.Z. Jumaat, N.B. Ghazali, S. Yusoff, I.I. Bashar, Influence of steel fibers on the mechanical properties and impact resistance of lightweight geopolymer concrete, Constr. Build. Mater. 152 (2017) 964–977.

[33] A. Bhutta, P.H.R.R. Borges, C. Zanotti, M. Farooq, N. Banthia, Flexural behavior of geopolymer composites reinforced with steel and polypropylene macro fibers, Cem. Concr. Compos. 80 (2017) 31–40.

[34] Z. Zheng, D. Feldman, Synthetic fibre-reinforced concrete, Prog. Polym. Sci. 20 (1995) 185–210.

[35] N. Banthia, R. Gupta, Influence of polypropylene fiber geometry on plastic shrinkage cracking in concrete, Cem. Concr. Res. 36 (2006) 1263–1267.

[36] S.M. Zabihi, H. Tavakoli, E. Mohseni, Engineering and microstructural properties of fiber-reinforced rice husk–ash based geopolymer concrete, J. Mater. Civ. Eng. 30 (2018) 4018183.

[37] T. Alomayri, I.M. Low, Synthesis and characterization of mechanical properties in cotton fiber-reinforced geopolymer composites, J. Asian Ceram. Soc. 1 (2013) 30–34.

[38] K. Korniejenko, E. Fraczek, E. Pytlak, M. Adamski, Mechanical properties of geopolymer composites reinforced with natural fibers, Proc. Eng. 151 (2016) 388–393.

[39] S. Alonso, A. Palomo, Alkaline activation of metakaolin and calcium hydroxide mixtures: influence of temperature, activator concentration and solids ratio, Mater. Lett. 47 (2001) 55–62.

[40] H. Baykara, M.H. Cornejo, R. Murillo, A. Gavilanes, C. Paredes, J. Elsen, Preparation, characterization and reaction kinetics of green cement: Ecuadorian natural mordenite-based geopolymers, Mater. Struct. 50 (2017) 188.

[41] M.H. Cornejo, J. Elsen, B. Togra, H. Baykara, G. Soriano, C. Paredes, Effect of calcium hydroxide and water to solid ratio on compressive strength of mordenite-based geopolymer and the evaluation of its thermal transmission property, in: Vol. 12 Mater. Genet. to Struct., ASME, 2018. V012T11A022.

[42] N.A. Ulloa, H. Baykara, M.H. Cornejo, A. Rigail, C. Paredes, J.L. Villalba, Application-oriented mix design optimization and characterization of zeolite-based geopolymer mortars, Constr. Build. Mater. 174 (2018) 138–149.

[43] J.L.V. Lynch, H. Baykara, M. Cornejo, G. Soriano, N.A. Ulloa, Preparation, characterization, and determination of mechanical and thermal stability of natural zeolite-based foamed geopolymers, Constr. Build. Mater. 172 (2018) 448–456.

[44] R.M. Hamidi, Z. Man, K.A. Azizli, Concentration of NaOH and the effect on the properties of fly ash based geopolymer, in: Procedia Eng., Elsevier B.V., 2016, pp. 189–193.

[45] ASTM C109/C109M-16a, Standard Test Method for Compressive Strength of Hydraulic Cement Mortars (Using 2-in. Or [50mm] Cube Specimens), 2016.

[46] P. Termkhajornkit, T. Nawa, M. Nakai, T. Saito, Effect of fly ash on autogenous shrinkage, Cem. Concr. Res. 35 (2005) 473–482.

[47] M.M. Al-mashhadani, O. Canpolat, Y. Aygörmez, M. Uysal, S. Erdem, Mechanical and microstructural characterization of fiber reinforced fly ash based geopolymer composites, Constr. Build. Mater. 167 (2018) 505–513.

[48] N. Ranjbar, S. Talebian, M. Mehrali, C. Kuenzel, H.S. Cornelis Metselaar, M.Z. Jumaat, Mechanisms of interfacial bond in steel and polypropylene fiber reinforced geopolymer composites, Compos. Sci. Technol. 122 (2016) 73–81.

[49] A. Cwirzen, J.L. Provis, V. Penttala, K. Habermehl-Cwirzen, The effect of limestone on sodium hydroxide-activated metakaolin-based geopolymers, Constr. Build. Mater. 66 (2014) 53–62.

[50] A. Aboulayt, M. Riahi, M. Ouazzani Touhami, H. Hannache, M. Gomina, R. Moussa, Properties of metakaolin based geopolymer incorporating calcium carbonate, Adv. Powder Technol. 28 (2017) 2393–2401.

[51] G.S. Ryu, Y.B. Lee, K.T. Koh, Y.S. Chung, The mechanical properties of fly ash-based geopolymer concrete with alkaline activators, Constr. Build. Mater. 47 (2013) 409–418.

[52] L. Yan, B. Kasal, L. Huang, A review of recent research on the use of cellulosic fibres, their fibre fabric reinforced cementitious, geo-polymer and polymer composites in civil engineering, Compos. Part B Eng. 92 (2016) 94–132.

[53] C. Ochoa-Putman, U.K. Vaidya, Mechanisms of interfacial adhesion in metal-polymer composites - effect of chemical treatment, Compos. Part A Appl. Sci. Manuf. 42 (2011) 906–915.

[54] N.U. Auqui, H. Baykara, A. Rigail, M.H. Cornejo, J.L. Villalba, An investigation of the effect of migratory type corrosion inhibitor on mechanical properties of zeolite-based novel geopolymers, J. Mol. Struct. 1146 (2017) 814–820.

[55] T. Alomayri, F.U.A. Shaikh, I.M. Low, Mechanical and thermal properties of ambient cured cotton fabric-reinforced fly ash-based geopolymer composites, Ceram. Int. 40 (2014) 14019–14028.

[56] M.A. Villaquirán-Caicedo, R.M. de Gutiérrez, S. Sulekar, C. Davis, J.C. Nino, Thermal properties of novel binary geopolymers based on metakaolin and alternative silica sources, Appl. Clay Sci. 118 (2015) 276–282.